

Citation for published version:

Jiang, DM, Burrows, AD & Edler, KJ 2011, 'Size-controlled synthesis of MIL-101(Cr) nanoparticles with enhanced selectivity for CO₂ over N₂', *CrystEngComm*, vol. 13, no. 23, pp. 6916-6919.
<https://doi.org/10.1039/c1ce06274c>

DOI:

[10.1039/c1ce06274c](https://doi.org/10.1039/c1ce06274c)

Publication date:

2011

Document Version

Peer reviewed version

[Link to publication](#)

University of Bath

Alternative formats

If you require this document in an alternative format, please contact:
openaccess@bath.ac.uk

General rights

Copyright and moral rights for the publications made accessible in the public portal are retained by the authors and/or other copyright owners and it is a condition of accessing publications that users recognise and abide by the legal requirements associated with these rights.

Take down policy

If you believe that this document breaches copyright please contact us providing details, and we will remove access to the work immediately and investigate your claim.

Cite this: DOI: 10.1039/c0xx00000x

www.rsc.org/xxxxxx

ARTICLE TYPE

Size-controlled synthesis of MIL-101(Cr) nanoparticles with enhanced selectivity for CO₂ over N₂

Dongmei Jiang, Andrew D. Burrows* and Karen J. Edler

Received (in XXX, XXX) Xth XXXXXXXXXX 20XX, Accepted Xth XXXXXXXXXX 20XX

DOI: 10.1039/b000000x

Nanoparticles of MIL-101(Cr) have been fabricated using a hydrothermal method for the first time. The particle size can be controlled from 19 (4) nm to 84 (12) nm, by using a monocarboxylic acid as a mediator. These nano MIL-101(Cr) materials exhibit higher selectivities for CO₂ over N₂ than bulk MIL-101(Cr).

Interest in nanoparticles, in which the particle size lies between 1 nm and 100 nm, has been growing steadily due to their unique position as a bridge between atoms and bulk solids.^{1,2} Nanoparticles possess additional physical and chemical properties to their bulk analogues due to their drastically increased surface to volume ratios. This in turn has promoted the development of new materials for various applications.

Metal-organic frameworks (MOFs) have generated great interest due to their intriguing structural properties such as high surface areas, and the rich diversities in their structures.³⁻⁵ This has led to many potential applications including gas storage, separations and catalysis.⁶ Nanocrystalline MOFs (NMOFs) possess the bulk phase properties of the MOF together with the additional physical/chemical properties derived from nanosized particles, and consequently can show improved properties.⁷ For example, enhanced H₂ heats of adsorption⁸ were found in the NMOF [Zn₄O(bdc)₃] (MOF-5, bdc = 1,4-benzenedicarboxylate). NMOFs have also been exploited as contrast agents in medical imaging techniques.⁹ Kitagawa and co-workers have demonstrated that for flexible MOFs, there can be structural differences between bulk MOFs and NMOFs.¹⁰ Despite this potential, research on the properties of NMOFs still lags behind that of their bulk counterparts, mainly due to the lack of general synthetic approaches.

Several specific strategies have been reported to synthesize nano MOFs.⁷ These include a reverse microemulsion methodology,¹¹ addition of a co-solvent into the reaction mixture,¹² use of microwaves^{13,14} or ultrasound,^{15,16} and addition of a modulator such as a polymer¹⁷ or surfactant.¹⁸ Simple dilution of the reaction mixture has been found to be effective in some cases.¹⁹ Although NMOFs with specific sizes can be obtained by the above methods, it is still challenging to finely control the particle sizes of NMOFs due to the complexity of the specific synthetic systems. Clearly, more control is required in the synthesis of NMOFs to enable their future applications to be systematically studied.

In the frameworks of MOFs, the organic linkers play a crucial

bridging role in the building up of the infinite network structure. Hence, organic ligands that are not capable of bridging can block the extension of the framework and thus provide the opportunity to regulate particle sizes. For carboxylate-based MOFs, monocarboxylic acids can be used to control particle size. It has been found that use of high concentrations of monocarboxylic acid in the syntheses restricts nucleation and enables large crystals to be formed.²⁰ In contrast, low concentrations of monocarboxylic acid allow control of the crystal growth, leading to small particles, with the monocarboxylate acting as an 'etching agent'.²¹ The acidities of monocarboxylic acids vary greatly, so we postulated that variation of the monocarboxylic acid used could provide a potential pathway for controlling particle size. Herein, we employ this approach to control the particle size of MOFs in the nanoscale regime and report the CO₂ sorption properties of the resultant nanomaterials.

[Cr₃OX(H₂O)₂(bdc)₃]·nH₂O (MIL-101(Cr), X = F, OH; n ~ 25) was selected as a model material. It has two types of zeotypic mesoporous pores with free diameters of *ca.* 2.9 and 3.4 nm accessible through two microporous windows of *ca.* 1.2 nm and 1.6 × 1.5 nm.²² A combination of the high mesoporosity and surface area of MIL-101(Cr) together with high thermal and chemical stability makes the material very promising for practical applications. The material was originally synthesised with Cr(NO₃)₃·9H₂O and H₂bdc under conventional hydrothermal conditions at 220 °C for 8 h using hydrofluoric acid (HF) as mineralising agent [Cr(NO₃)₃·9H₂O : H₂bdc : HF : 265H₂O]. Compared to other MOFs, the particle sizes of MIL-101(Cr) are smaller (down to 1 µm), but still much larger than nanocrystals. Serre and co-workers showed that 22 nm nanoparticles of MIL-101(Cr) could be prepared by microwave heating without HF.²³ Jung and co-workers have recently demonstrated that dilution can lower the MIL-101(Cr) particle size to 200 nm, and they also prepared nanoparticles using microwave heating.¹⁹

By optimising the reaction parameters, we were able to prepare nanoparticles of MIL-101(Cr) hydrothermally from the diluted reagent mixture at 180 °C for 4 h [Cr(NO₃)₃·9H₂O : H₂bdc : 1680H₂O] without addition of hydrofluoric acid, as shown in Fig. 1a. The nanoparticles take multifaceted sphere shapes, and a particle size analysis revealed that the nanoparticles were relative homogeneous, with an average size of 50 nm. Importantly, the nanoparticles were prepared in good yield (49 %) and the results are fully reproducible.

For further control of the particle sizes, low concentrations (30

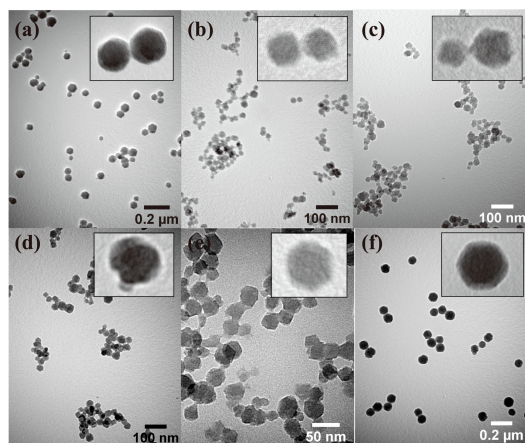


Fig. 1 TEM images of the NMOFs with/without chemical additives: (a) no additive; (b) stearic acid; (c) 4-methoxybenzoic acid; (d) benzoic acid; (e) 4-nitrobenzoic acid; (f) perfluorobenzoic acid.

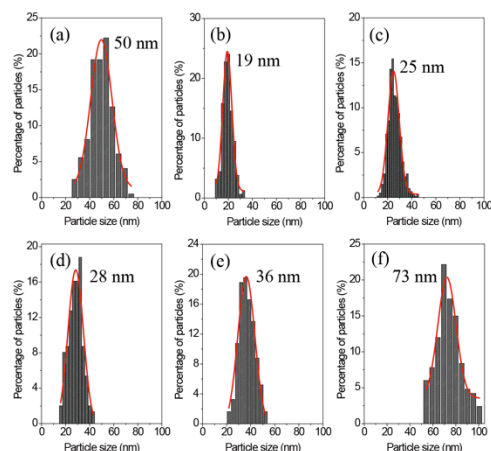


Fig. 2 Particle size distribution of the NMOFs with/without chemical additives: (a) no additive; (b) stearic acid; (c) 4-methoxybenzoic acid; (d) benzoic acid; (e) 4-nitrobenzoic acid; (f) perfluorobenzoic acid.

mol% based on H_2bdc) of the monocarboxylic acids stearic acid, benzoic acid, 4-methoxybenzoic acid, 4-nitrobenzoic acid and perfluorobenzoic acid, were introduced separately into the synthetic system from which the 50 nm nanoparticles were obtained. TEM images (Fig. 1) show that the nanoparticles synthesised with the monocarboxylic acid modulators have similar multifaceted sphere shapes to those synthesised in their absence. The nanoparticles have average particle sizes of 19 nm, 25 nm, 28 nm, 36 nm and 73 nm with stearic, 4-methoxybenzoic, benzoic, 4-nitrobenzoic and perfluorobenzoic acids respectively (Fig. 2), demonstrating that addition of a monocarboxylic acid enables the size distributions to be controlled.

There are a number of factors that could influence the nanoparticle sizes. It has previously been observed that the amount of monocarboxylic acid added could be used to control the particle size and morphology of nano $[Cu_3(btc)_2]$.²⁰ In our case, the change in particle size occurs with the same concentration of monocarboxylic acids, which suggests that the nature of the carboxylic acid is important. Indeed, the particle sizes observed are well correlated to the pK_a values of the monocarboxylic acids (Table 1), with lower pK_a leading to larger nanoparticles. The lower the pK_a , the higher the concentration of the monocarboxylate in solution. This could lead to suppression

Table 1 Physicochemical data for the nano MIL-101(Cr) materials

Carboxylic acid additive	pK_a^a	Particle size ^b /nm	S_{BET}^c /m ² g ⁻¹	V_{total}^d /m ³ g ⁻¹
None	--	50 (9)	2944	2.57
Stearic acid	10.15	19 (4)	2691	2.95
4-Methoxybenzoic acid	4.49	25 (6)	2646	2.68
Benzoic acid	4.19	28 (6)	2923	2.93
4-Nitrobenzoic acid	3.44	36 (7)	2692	2.53
Perfluorobenzoic acid	1.60	73 (8)	2893	2.33

^a pK_a at 25 °C in water, ^b The average particle size was analysed using a gaussian model and estimated standard deviations are given in brackets,

^c The specific surface area was calculated in the P/P_0 range of 0.05-0.1. ^d The total volume was calculated by taking the data at P/P_0 0.99.

of nucleation, leading to larger particle sizes. In order to assess whether the general trend holds, the synthesis was carried out with perfluorostearic acid, for which pK_a 0.6. This is more acidic than the other monocarboxylic acids used in the syntheses, so would be expected to lead to larger nanoparticles. This was indeed observed, with use of this acid in the synthesis leading to an average particle size of 84 nm (Fig. S1 and S2). Similar trends have also been found for nanoTiO₂ on re-analysis of results from Yin and co-workers.²⁴

The crystal structure and porosity of the nanomaterials synthesised with and without monocarboxylic acids were further investigated by X-ray powder diffraction (XRD) and N₂ sorption. The XRD patterns of all samples (Fig. 3) are similar to the simulated pattern of MIL-101(Cr) reported previously,²⁵ confirming the crystal structure of the samples. The broad Bragg reflections of the XRD patterns of the samples are attributed to the small particle size effects, and indeed the lines get broader as the nanoparticle size decreases. Fig. 4 shows the N₂ adsorption-desorption isotherms of the samples at 77 K after evacuation of the samples at 150 °C for 4 h. The nano MIL-101(Cr) materials exhibited similar Type I isotherms to that reported for MIL-101(Cr)²⁵ with $P/P_0 < 0.8$. The two uptake steps near $P/P_0 = 0.1$ and $P/P_0 = 0.2$ reflect the presence of two kinds of microporous windows in the structure. The pore size distribution curves (calculated by using BJH equation) of the nano MIL-101(Cr) materials (Fig. 4) shows two different monodisperse pore sizes, 1.6 and 2.1 nm, which are similar to the pore sizes estimated from the crystal structure. Interestingly, the nano MIL-101(Cr) materials show increased nitrogen uptakes in the high relative

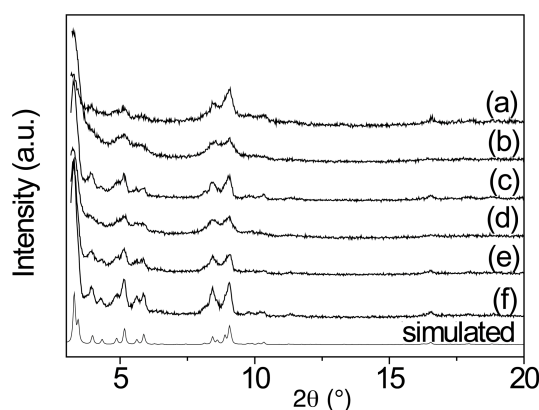


Fig. 3 XRD patterns of the NMOFs with/without chemical additives: (a) no additive; (b) stearic acid; (c) 4-methoxybenzoic acid; (d) benzoic acid; (e) 4-nitrobenzoic acid; (f) perfluorobenzoic acid. The pattern simulated from the crystal structure of MIL-101(Cr) is shown for comparison.

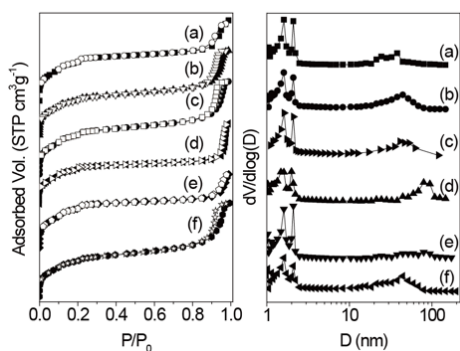


Fig. 4 N₂ adsorption-desorption isotherms (left) and pore size distribution curves (right) of the NMOFs with/without chemical additives at 77 K: (a) no additive; (b) stearic acid; (c) 4-methoxybenzoic acid; (d) benzoic acid; (e) 4-nitrobenzoic acid; (f) perfluorobenzoic acid.

pressure region of the adsorption isotherm branch with large hysteresis loops. This phenomenon is related to the physisorbed nitrogen on the outer surfaces of the nanoparticles leading to textural porosities in the nano MIL-101(Cr) solid materials. The nano MIL-101(Cr) materials not only have high specific surface areas (2646 to 2944 m² g⁻¹, Table 1), but also have higher total pore volumes of 2.33 to 2.95 cm³ g⁻¹, which compare with the best value of 2.15 cm³ g⁻¹ in the literature.²⁶

CO₂ sorption properties of the nano MIL-101(Cr) materials under low pressure were studied at 273 K. Before N₂ and CO₂ uptake measurements, the materials were activated by a two step process using hot ethanol and aqueous NH₄F solutions. As mentioned previously, the activation of MIL-101(Cr) is of crucial importance.²⁶ It was observed again here that the activation improved the CO₂ uptakes of the nano MIL-101(Cr) (Fig. S4), which was mainly attributed to the removal of trace amounts of free H₂bdc from the pores. Table 2 further gives the CO₂ uptakes and selectivities over N₂ of the nano MIL-101(Cr) materials (Fig. S5). All of the nano MIL-101(Cr) materials show high CO₂ uptakes of 5.27 to 4.60 mmol g⁻¹, except that synthesised with stearic acid which is mainly due to the decreased surface area (1970 vs 2691 cm² g⁻¹) and total pore volume (1.16 vs 2.95 cm³ g⁻¹) after activation (Fig. S3). Because the crystallinity, surface area and pore volume of the material can have large influences on the absolute gas uptake, it is often more valuable to compare the selectivities of the materials. Also the selectivity is important to evaluate the material for gas separation. The nano MIL-101(Cr) materials show higher selectivities for CO₂ over N₂ than the bulk

Table 2 CO₂ and N₂ adsorption data for the activated nano MIL-101(Cr) materials under 1 atm at 273 K

Carboxylic acid (CA) additive	CA/H ₂ bdc ^a mol:mol	CO ₂ /mmol g ⁻¹	N ₂ /mmol g ⁻¹	Selectivity ^b
None	—	5.27	0.71	7.4
Stearic acid	0.017:1	3.35	0.35	9.6
4-Methoxybenzoic acid	0.041:1	4.87	0.55	8.9
Benzoic acid	0.015:1	5.17	0.67	7.7
4-Nitrobenzoic acid	0.023:1	5.11	0.54	9.5
Perfluorobenzoic acid	—	4.60	0.58	7.9
Bulk MIL-101	—	5.54	0.78	7.1

^a The molar ratio of CA to H₂bdc in the material was measured by ¹H NMR spectroscopy of the digested product. ^b The selectivity was calculated from the single gas isotherms by dividing the CO₂ adsorption capacity by that of N₂.

material, which is probably due to the nature of the functional groups on the surface of the nano MIL-101(Cr) materials. Depending on the monocarboxylic acid used, the selectivity of the nano MIL-101(Cr) materials can be increased by between 8% and 35%. ¹H NMR measurements on the digested solids, made by dissolving the nano MIL-101(Cr) materials in basic D₂O solution, further show that the molar ratio of monocarboxylate groups to 1,4-benzenedicarboxylate groups in the nano MIL-101(Cr) materials varied from 0.015:1 to 0.041:1.

In summary, we have demonstrated that nanoparticles of MIL-101(Cr) can be prepared hydrothermally and that their particle size can be adjusted through judicious choice of a monocarboxylic acid modulator. This provides a new strategy to control NMOF particle size, and current work involves extending this study to other MOF systems in order to assess the generality of the approach. In addition, the monocarboxylic acids also functionalise the nanoparticle surfaces, which modifies their gas adsorption properties. This provides a simple means of producing functionalised NMOFs.

The EPSRC are acknowledged for financial support.

Notes and references

- ^aDepartment of Chemistry, University of Bath, Claverton Down, Bath BA2 9Y, UK. Fax: +44 (0)1225 386231; Tel: +44 (0) 1225 386529; E-mail: a.d.burrows@bath.ac.uk
- † Electronic Supplementary Information (ESI) available: Syntheses, TEM, N₂ and CO₂ sorption data. See DOI: 10.1039/b000000x/
1. E. Roduner, *Chem. Soc. Rev.*, 2006, **35**, 583.
2. Y. Li and G. A. Somorjai, *Nano Lett.*, 2010, **10**, 2289.
3. D. J. Tranchemontagne, J. L. Mendoza-Cortés, M. O'Keeffe and O. M. Yaghi, *Chem. Soc. Rev.*, 2009, **38**, 1257.
4. G. Férey, *Chem. Soc. Rev.*, 2008, **37**, 191.
5. S. Horike, S. Shimomura and S. Kitagawa, *Nature Chem.*, 2009, **1**, 695.
6. A. U. Czaja, N. Trukhan and U. Müller, *Chem. Soc. Rev.*, 2009, **38**, 1284.
7. A. Carné, C. Carbonell, I. Imaz and D. MasPOCH, *Chem. Soc. Rev.*, 2011, **40**, 291.
8. Z. Xin, J. Bai, Y. Pan and M. J. Zaworotko, *Chem. Eur. J.*, 2010, **16**, 13049.
9. J. Della Rocca and W. Lin, *Eur. J. Inorg. Chem.*, 2010, 3725.
10. Y. Hijikata, S. Horike, D. Tanaka, J. Groll, M. Mizuno, J. Kim, M. Takata and S. Kitagawa, *Chem. Commun.*, 2011, **47**, 7632.
11. W. J. Rieter, K. M. L. Taylor, H. An, W. Lin and W. Lin, *J. Am. Chem. Soc.*, 2006, **128**, 9024.
12. W. J. Rieter, K. M. Pott, K. M. L. Taylor and W. Lin, *J. Am. Chem. Soc.*, 2008, **130**, 11584.
13. T. Chalati, P. Horcajada, R. Gref, P. Couvreur and C. Serre, *J. Mater. Chem.*, 2011, **21**, 2220.
14. D. Liu, R. C. Huxford and W. Lin, *Angew. Chem. Int. Ed.*, 2011, **50**, 3696.
15. L. G. Qiu, Z. Q. Li, Y. Wu, W. Wang, T. Xu and X. Jiang, *Chem. Commun.*, 2008, 3642.
16. D. Tanaka, A. Henke, K. Albrecht, M. Moeller, K. Nakagawa, S. Kitagawa and J. Groll, *Nature Chem.*, 2010, **2**, 410.
17. D. Jiang, T. Mallat, F. Krumeich and A. Baiker, *Catal. Commun.*, 2011, **12**, 602.
18. K. M. L. Taylor, A. Jin and W. Lin, *Angew. Chem. Int. Ed.*, 2008, **47**, 7722.
19. N. A. Khan, I. J. Kang, H. Y. Seok and S. H. Jung, *Chem. Eng. J.*, 2011, **166**, 1152.
20. S. Diring, S. Furukawa, Y. Takashima, T. Tsuruoka and S. Kitagawa, *Chem. Mater.*, 2010, **22**, 4531.

-
21. S. Hermes, T. Witte, T. Hikov, D. Zacher, S. Bahn Müller, G. Langstein, K. Huber and R. A. Fischer, *J. Am. Chem. Soc.*, 2007, **129**, 5324.
22. G. Férey, C. Mellot-Draznieks, C. Serre, F. Millange, J. Dutour, S. Surblé and I. Margiolaki, *Science*, 2005, **309**, 2040.
23. A. Demessence, P. Horcajada, C. Serre, C. Boissière, D. Grosso, C. Sanchez and G. Férey, *Chem. Commun.*, 2009, 7149.
24. B. Jiang, H. Yin, T. Jiang, J. Yan, Z. Fan, C. Li, J. Wu and Y. Wada, *Mater. Chem. Phys.*, 2005, **92**, 595.
25. D.-Y. Hong, Y. K. Hwang, C. Serre, G. Férey and J.-S. Chang, *Adv. Funct. Mater.*, 2009, **19**, 1537.
26. P. L. Llewellyn, S. Bourrelly, C. Serre, A. Vimont, M. Daturi, L. Hamon, G. De Weireld, J.-S. Chang, D.-Y. Hong, Y. K. Hwang, S. H. Jhung and G. Férey, *Langmuir*, 2008, **24**, 7245.

15